nature immunology

Diverse intracellular pathogens activate type III interferon expression from peroxisomes

Charlotte Odendall[1], Evelyn Dixit[1,7], Fabrizia Stavru[2,7], Helene Bierne[2,6], Kate M Franz[1], Ann Fiegen Durbin[3,4], Steeve Boulant[5], Lee Gehrke[3,4], Pascale Cossart[2] & Jonathan C Kagan[1]

Type I interferon responses are considered the primary means by which viral infections are controlled in mammals. Despite this view, several pathogens activate antiviral responses in the absence of type I interferons. The mechanisms controlling type I interferon–independent responses are undefined. We found that RIG-I like receptors (RLRs) induce type III interferon expression in a variety of human cell types, and identified factors that differentially regulate expression of type I and type III interferons. We identified peroxisomes as a primary site of initiation of type III interferon expression, and revealed that the process of intestinal epithelial cell differentiation upregulates peroxisome biogenesis and promotes robust type III interferon responses in human cells. These findings highlight the importance of different intracellular organelles in specific innate immune responses.

In mammals, antiviral responses are classically defined as being mediated by type I interferons. These secreted proteins act via interferon receptors to upregulate interferon-stimulated genes (ISGs) that exhibit diverse antiviral activities[1]. Despite this paradigm, there are several examples of infections that induce expression of ISGs independently of type I interferons[2–5]. The mechanisms by which these type I interferon–independent activities are induced remain unclear. One such example comes from studies of the signaling events mediated by RLRs[2]. RLRs are RNA helicases that function in virtually all mammalian cells to detect viral and bacterial nucleic acids in the cytosol[6]. The two best-characterized RLRs are RIG-I and Mda5, which differ mainly in their ability to recognize distinct RNA structures. RIG-I detects short double-stranded RNA that contains a 5′ triphosphate group, and Mda5 detects long double-stranded RNA structures[6]. These distinct recognition profiles are thought to explain the importance of each RLR in the detection of different classes of viral pathogens[7].

Upon detection of viral RNA, RLRs engage an adaptor protein called MAVS (also known as IPS-1, Cardif or VISA)[8], which is located on the limiting membranes of mitochondria, peroxisomes and mitochondria-associated membranes of the endoplasmic reticulum[2,8,9]. Engagement of MAVS by RLRs activates a signaling cascade that induces numerous antiviral activities[10]. Mitochondria-localized MAVS induces an antiviral response typified by the expression of type I interferons and ISGs. In contrast, RLR signaling via MAVS on peroxisomes does not induce the expression of any type I interferon but does induce expression of ISGs[2]. This atypical antiviral response is functional, as cells expressing MAVS exclusively on peroxisomes restrict the replication of two mammalian RNA viruses, reovirus and vesicular stomatitis virus (VSV). Thus, although it is clear that type I interferon–independent mechanisms of antiviral immunity exist, the regulation of these mechanisms remains largely undefined. This lack of information represents a fundamental gap in our knowledge of the means by which mammalian cells respond to intracellular pathogens.

Here we report that RLR signaling in human cells can induce the expression of type III interferons, a class of interferons that has tissue-specific roles in antiviral immunity[11]. We found that RLR-mediated type III interferon expression can be induced by diverse viruses, including reovirus, Sendai virus (SeV) and dengue virus (DenV) as well as the bacterial pathogen *Listeria monocytogenes*. We identified peroxisomes as signaling organelles that act to induce type III interferon–mediated ISG responses, which complement the actions of the type I interferon responses induced from mitochondria. During the natural process of epithelial cell differentiation and polarization, we observed an increase in the type III interferon response that correlated with abundance of peroxisomes, and cells derived from individuals with peroxisomal disorders displayed aberrant antiviral responses. These data establish the importance of peroxisomes in controlling interferon responses and highlight the interconnectedness of the RLR pathways with the metabolic organelles of mammalian cells.

RESULTS

Jak-STAT–dependent RLR signaling from peroxisomes

Type I interferons are neither detected nor required for antiviral responses induced by RLRs from peroxisomes[2], which suggests a

[1]Harvard Medical School and Division of Gastroenterology, Boston Children's Hospital, Boston, Massachusetts, USA. [2]Institut Pasteur, Unité des Interactions Bactéries Cellules, Institut National de la Santé et de la Recherche Médicale U604, Institut national de la recherche agronomique (INRA) USC2020, Paris, France. [3]Department of Microbiology and Immunobiology, Harvard Medical School, Boston, Massachusetts, USA. [4]Institute for Medical Engineering and Science, Massachusetts Institute of Technology, Cambridge, Massachusetts, USA. [5]Department of Infectious Diseases, Virology Schaller research group at CellNetworks and Deutsches Krebsforschungszentrum (DKFZ), University of Heidelberg, Heidelberg, Germany. [6]Present address: INRA, Unité mixte de recherche (UMR) 1319 Micalis, Jouy-en-Josas, France, and AgroParis Tech, UMR Micalis, Jouy-en-Josas, France. [7]These authors contributed equally to this work. Correspondence should be addressed to J.C.K. (jonathan.kagan@childrens.harvard.edu).

Received 7 March; accepted 6 May; published online 22 June 2014; doi:10.1038/ni.2915

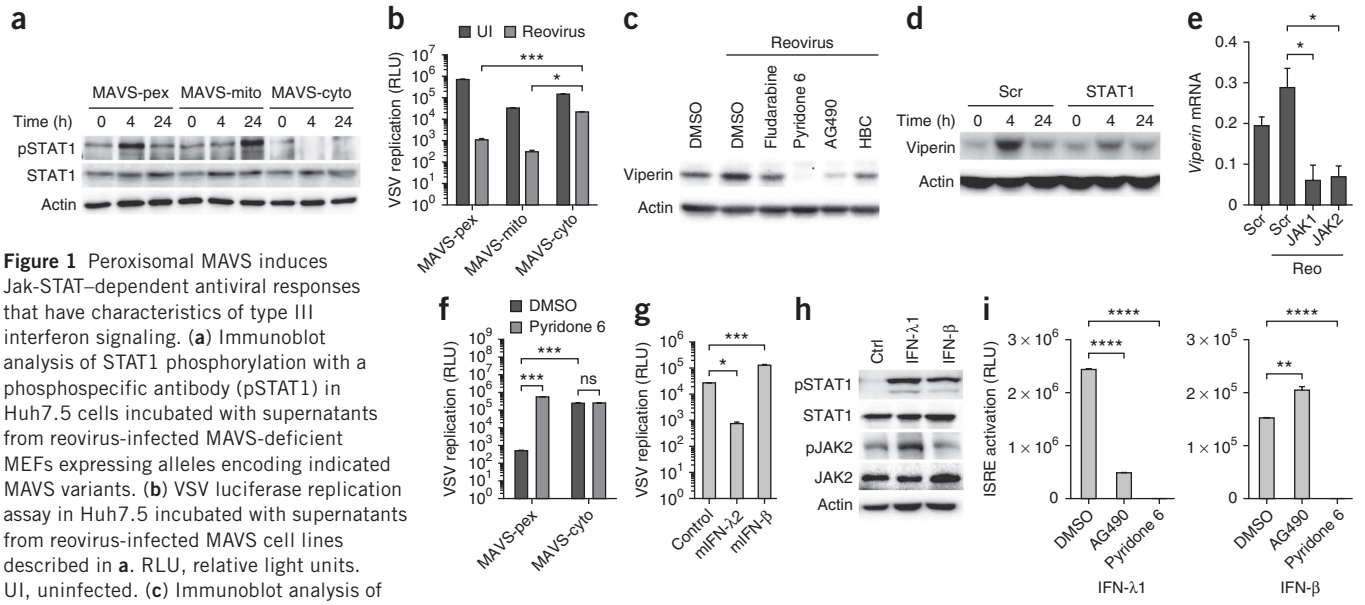

Figure 1 Peroxisomal MAVS induces Jak-STAT–dependent antiviral responses that have characteristics of type III interferon signaling. (**a**) Immunoblot analysis of STAT1 phosphorylation with a phosphospecific antibody (pSTAT1) in Huh7.5 cells incubated with supernatants from reovirus-infected MAVS-deficient MEFs expressing alleles encoding indicated MAVS variants. (**b**) VSV luciferase replication assay in Huh7.5 incubated with supernatants from reovirus-infected MAVS cell lines described in **a**. RLU, relative light units. UI, uninfected. (**c**) Immunoblot analysis of viperin in MAVS-deficient MEFs expressing MAVS-pex, treated with 50 μM fludarabine, 2 μM pyridone 6, 50 μM AG490 or 50 μM HBC and infected with reovirus for 4 h. (**d**) Immunoblot analysis of viperin in MAVS-deficient MEFs expressing MAVS-pex transfected with a scrambled (Scr) or *STAT1* siRNA oligo (STAT1) and subsequently infected with reovirus for the durations indicated. (**e**) *Viperin* quantitative reverse transcription real-time PCR (qRT-PCR) of reovirus-infected MAVS-deficient MEFs expressing MAVS-pex and depleted of JAK1 or JAK2 or transfected with a scrambled (Scr) siRNA oligo. (**f**) Luciferase assay of MAVS-pex or MAVS-cyto MEFs treated with the pan-Jak inhibitor pyridone 6 and infected with VSV expressing luciferase. (**g**) Luciferase assay of Huh7.5 cells incubated with mouse IFN-λ2 (mIFN-λ2) or IFN-β (mIFN-β) and subsequently infected with VSV expressing luciferase. (**h**) Immunoblot analyses of STAT1 and JAK2 phosphorylation in Huh7.5 cells treated with human IFN-λ1 or IFN-β for 2 h. (**i**) Luciferase analysis of 293T cells expressing luciferase under the control of an *ISRE* promoter treated with the Jak2 inhibitor AG490 or the pan-Jak inhibitor pyridone 6, and incubated with human IFN-λ1 or IFN-β. Data are representative of two experiments (**h**), three experiments (**a**,**b**,**e**–**g**,**i**; error bars, s.d. in **b**,**f**,**g**,**i** and s.e.m. in **e**; $n = 3$ technical replicates) or four experiments (**c**,**d**). $^{*}P < 0.05$; $^{**}P < 0.01$; $^{***}P < 0.0001$; ns, not significant (one-way ANOVA).

cell-intrinsic means of antiviral immunity. Cell-intrinsic responses are considered those that do not involve the actions of secreted factors. To determine whether cellular responses induced from peroxisomes induce the secretion of any antiviral factors, we used previously characterized MAVS-deficient mouse embryonic fibroblasts (MEFs)[2]. These MEFs stably express MAVS transgenes that had been engineered to be localized to specific organelles. The resulting isogenic cell populations only differ in that they display MAVS on mitochondria (MAVS-mito), on peroxisomes (MAVS-pex) or in the cytosol (MAVS-cyto). We infected these cells with mammalian reovirus (a physiological activator of RLRs) and transferred culture supernatants from infected cells onto Huh7.5 human hepatocyte-like cells. Huh7.5 cells are an Huh7 derivative that carries a loss-of-function mutation in RIG-I[12]. We assessed the antiviral activity of the supernatants by monitoring phosphorylation of the transcription factor STAT1. The fact that Huh7.5 cells are deficient for RIG-I signaling ensures that a response would be due to MEF secretion in the supernatant and not carryover virus. Culture supernatants from infected MAVS-pex and MAVS-mito MEFs activated phosphorylation of STAT1 in Huh7.5 cells (**Fig. 1a**). In contrast, supernatants from cells expressing the signaling-defective 'MAVS-cyto' allele[2,8] could not trigger phosphorylation of STAT1, which indicated that these supernatants did not contain any STAT1 activators. This finding suggested that peroxisomal MAVS can activate cell-extrinsic antiviral responses, despite its inability to induce type I interferon expression[2].

To determine whether the secreted factor(s) were truly antiviral, we allowed the same culture supernatants to stimulate Huh7.5 cells for 8 h, at which time we infected the cells with VSV. We chose VSV for these studies because its ability to replicate is highly sensitive to the actions of interferons. Compared to supernatants collected from uninfected MEFs, culture supernatants from reovirus-infected MAVS-pex or MAVS-mito MEFs restricted the replication of VSV by 100–1,000-fold (**Fig. 1b**). As expected from the lack of STAT1 phosphorylation, culture supernatants from MAVS-cyto cells exhibited minimal antiviral activity. These results indicate that MAVS signaling from either mitochondria or peroxisomes induces secretion of antiviral activities that activate STAT1.

To determine whether STAT1 is required for antiviral responses induced from peroxisomes, we treated MAVS-pex MEFs with the small-molecule inhibitor of STAT1, fludarabine[13]. In response to reovirus infection, protein expression of the well-characterized ISG Rsad2 (also known as viperin) was blocked by fludarabine (**Fig. 1c**). Small interfering (si)RNA–mediated knockdown of STAT1 also revealed a requirement for this transcription factor in the ability of MAVS-pex to induce expression of viperin (**Fig. 1d** and **Supplementary Fig. 1a**). STAT1 activation is classically governed by Jak kinases[14]. To determine whether Jak signaling was also required for the antiviral responses activated from peroxisomes, we used the pan-Jak inhibitor pyridone 6 and the Jak2 inhibitors AG490 and 1,2,3,4,5,6-hexabromocyclohexane (HBC)[15,16]. All these inhibitors blocked the induction of viperin in response to reovirus in MAVS-pex MEFs (**Fig. 1c**). Small interfering (si)RNA-mediated knockdown of Jak1 or Jak2 also revealed a requirement for these kinases in the ability of MAVS-pex to induce expression of *viperin* mRNA (**Fig. 1e** and **Supplementary Fig. 1b**). Moreover, the pan-Jak inhibitor pyridone 6 blocked the ability of MAVS-pex MEFs to control replication of VSV (**Fig. 1f**). These data establish that MAVS signaling from peroxisomes induces the secretion of Jak-STAT1–dependent activities and that these activities are required to create an antiviral cellular state.

RLR-dependent expression and activities of type III interferons

The experiments described above revealed that MAVS signaling from either peroxisomes or mitochondria induces secretion of antiviral factors. These factors must be cross-reactive between species because MEFs and Huh7 cells are of mouse and human origin, respectively. This point is notable because the cellular responses to type I interferons are species-specific[17]. For example, recombinant mouse IFN-β did not restrict VSV replication in human cells (**Fig. 1g**). Moreover, type I interferon signaling does not involve Jak2 (ref. 18), yet Jak2-specific inhibitors (AG490 and HBC) and siRNAs blocked the antiviral actions of this secreted factor (**Fig. 1c**,**e**). These experiments verify that signaling from peroxisomal MAVS does not induce secretion of type I interferon and indicate that the secreted factor of interest must be one that crosses species and exhibits antiviral activities that involve Jak2.

Although the antiviral activities of type I interferons cannot cross species, those of type III interferons can do so. For example, recombinant mouse type III interferon (also known as IFN-λ family or IL28-29, here referred to as IFN-λ2) induced phosphorylation of STAT1 (**Supplementary Fig. 1c**), activation of interferon-stimulated response element (ISRE; **Supplementary Fig. 1d**) and protection from VSV infection in human cells (**Fig. 1g**). Mouse IFN-β exhibited none of these antiviral activities on human cells (**Fig. 1g** and **Supplementary Fig. 1c**,**d**), as expected[17,19]. We found that recombinant human IFN-λ1 (but not IFN-β) induced phosphorylation of Jak2 (**Fig. 1h**), as reported[20], and the ability of IFN-λ1 to activate ISRE-based reporter genes was blocked by a pan-Jak inhibitor and by the Jak2-specific inhibitor AG490 (**Fig. 1i**). Type I interferon signaling was not blocked by AG490 (**Fig. 1i**). Thus, type III interferons exhibit all the properties of the factor secreted after MAVS signaling from peroxisomes.

In contrast to our understanding of type I interferon gene expression, the mechanisms governing type III interferon expression are not understood[21]. Type III interferons are produced in response to many viruses, similar to type I interferons[11]. Little is known about what differentiates the signaling pathways that lead to type I versus type III interferon gene expression, and most studies have focused on the similarities between these two interferon systems[22,23]. A major hurdle to understanding the regulation of type III interferon expression is that the most highly inducible family member in humans (IFN-λ1, also known as IL-29) is a pseudogene in mice[24]. Differences in expression (and function) of the type III interferon receptor have also been reported in human versus mouse livers[25]. Thus, although the type III interferon genes are functional in mice, they are less well-expressed and difficult to study experimentally[23,26]. This difficulty in detecting type III interferon expression has hindered the use of mouse models to dissect the signaling pathways that control these antiviral genes. Thus, we used human cells to define the signaling pathways that regulate type III interferon expression, as humans encode a functional and highly inducible IFN-λ1 (ref. 11).

We tested the ability of a variety of primary cell types and laboratory cell lines to produce type I and type III interferons in response to a range of pathogens. We used mucosal epithelial and stromal cells of human origin because these cells express the highest levels of the type III interferon receptor[27], and type III interferon signaling is required to control infections by mucosal pathogens[28]. We examined encounters between pathogens and the cell types they infect naturally (e.g., dengue virus in hepatocytes) and also used well-described activators of the RLR pathway, such as SeV. Infection of primary human hepatocytes, bronchial epithelial cells (BECs), keratinocytes, myoblasts, peripheral blood mononuclear cells (PBMCs) or monocytes with a range of viral pathogens resulted in the coincident expression of mRNA encoding IFN-λ1 (*IFNL1*) and IFN-β (*IFNB1*) (**Fig. 2a**).

In primary cells, basal levels of mRNA encoding IFN-λ were far lower than those for IFN-β. For this reason, here we did not present the inducible expression of interferon genes as a 'fold induction' value, but rather as compared to the expression of the housekeeping gene *GAPDH*. In T84 colonic epithelial cells, expression of type III interferon was induced at least as well as that of type I interferon in response to reovirus (**Fig. 2b**). Huh7 hepatocytes also revealed that type III interferon expression coincides with type I interferon expression after infection with SeV (**Fig. 2c**) or DenV (**Fig. 2d**), the latter being a natural pathogen of hepatocytes[29]. To our surprise, Huh7 cells did not express any class of interferon genes in response to infection by the bacterial pathogen *L. monocytogenes,* but infection of Jeg3 trophoblasts, a natural target cell type of *Listeria* species infections, revealed a strong type III interferon response (**Fig. 2e**), consistent with our previous data[30,31]. These data indicate that expression of type III interferons is a common feature of the antimicrobial responses that operate in human cells.

To understand the importance of type III interferons in the antiviral activities of human cells, we used neutralizing antibodies to the type I interferon receptor (IFNAR), the type III interferon receptor (IFNλR) or a combination of both in T84 intestinal epithelia. 5 h after infection with reovirus, neutralization of the IFNλR strongly reduced the ability of T84 cells to produce the ISGs *RSAD2* (here referred to as *viperin*) or *IFIT1* (**Fig. 2f**). At that time, IFNAR-neutralizing antibodies were less effective than the IFNλR-neutralizing antibodies at influencing expression of ISGs. 24 h after infection, the effectiveness of the neutralizing antibodies was diminished. Nevertheless, the early disruption of ISG expression was functionally important, as type III interferon signaling was necessary to control reovirus mRNA expression: neutralization of IFNλR resulted in more reovirus transcripts as compared to neutralization of IFNAR (**Fig. 2g**). To complement these studies on receptor neutralization, we used inhibitors of the Jak-STAT pathway to determine their effect on ISG expression. Inhibitors of STAT1 (fludarabine) or Jak2 (AG490) blocked the induction of *viperin* mRNA (**Supplementary Fig. 2a**) and other ISGs (**Fig. 2h**) to a similar extent, whereas the pan-Jak inhibitor pyridone 6 nearly abolished ISG expression (**Fig. 2h** and **Supplementary Fig. 2a**). As Jak2 inhibitors only block type III interferon signaling, these data suggest that type III interferon signaling controls antiviral gene expression, even when type I interferons are expressed.

Common and distinct regulators of IFN-β and IFN-λ

In MEFs, the RLR pathway has been implicated in the control of type III interferon expression[22]. The aforementioned limitations of the mouse system to study type III interferon expression prompted us to reexamine this question. To investigate the pathway that drives type III interferon expression in human cells, we determined whether the RLR-MAVS pathway is required for production of *IFNL1* mRNA in response to intracellular pathogens. We used Huh7 cells for these studies because they are easy to manipulate and are widely used to study host-pathogen interactions. We studied the involvement of RIG-I in type III interferon signaling using RIG-I–deficient Huh7.5. Infection with SeV revealed that RIG-I is required for production of *IFNL1* as well as *IFNB1* mRNA (**Fig. 3a**). siRNA-mediated knockdown of MAVS (**Supplementary Fig. 2b**) also inhibited production of both interferon types in response to SeV (**Fig. 3b**) and the natural pathogen of hepatocytes, DenV (**Fig. 3c**)[29]. To determine whether MAVS has a role in bacteria-mediated expression of type III interferon, we infected Jeg3 placental trophoblasts with

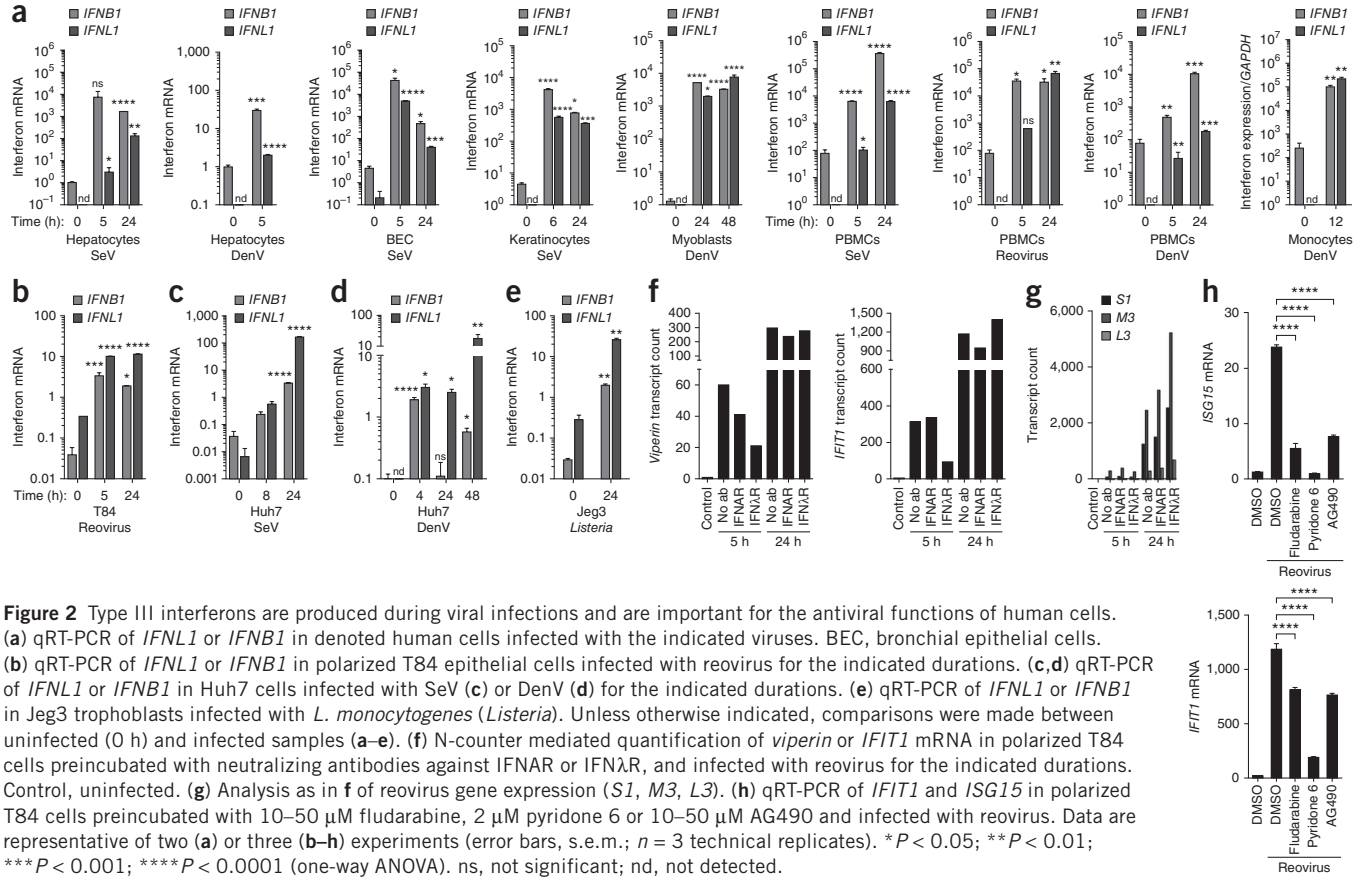

Figure 2 Type III interferons are produced during viral infections and are important for the antiviral functions of human cells. (**a**) qRT-PCR of *IFNL1* or *IFNB1* in denoted human cells infected with the indicated viruses. BEC, bronchial epithelial cells. (**b**) qRT-PCR of *IFNL1* or *IFNB1* in polarized T84 epithelial cells infected with reovirus for the indicated durations. (**c**,**d**) qRT-PCR of *IFNL1* or *IFNB1* in Huh7 cells infected with SeV (**c**) or DenV (**d**) for the indicated durations. (**e**) qRT-PCR of *IFNL1* or *IFNB1* in Jeg3 trophoblasts infected with *L. monocytogenes* (*Listeria*). Unless otherwise indicated, comparisons were made between uninfected (0 h) and infected samples (**a**–**e**). (**f**) N-counter mediated quantification of *viperin* or *IFIT1* mRNA in polarized T84 cells preincubated with neutralizing antibodies against IFNAR or IFNλR, and infected with reovirus for the indicated durations. Control, uninfected. (**g**) Analysis as in **f** of reovirus gene expression (*S1*, *M3*, *L3*). (**h**) qRT-PCR of *IFIT1* and *ISG15* in polarized T84 cells preincubated with 10–50 μM fludarabine, 2 μM pyridone 6 or 10–50 μM AG490 and infected with reovirus. Data are representative of two (**a**) or three (**b**–**h**) experiments (error bars, s.e.m.; $n = 3$ technical replicates). $^{*}P < 0.05$; $^{**}P < 0.01$; $^{***}P < 0.001$; $^{****}P < 0.0001$ (one-way ANOVA). ns, not significant; nd, not detected.

L. monocytogenes. Knockdown experiments (**Supplementary Fig. 2c**) revealed that MAVS is required for the efficient expression of type III interferons in addition to type I interferons during infection by *L. monocytogenes* (**Fig. 3d**). These collective data indicate that the RLR-MAVS pathway regulates the expression of both classes of interferons in various human cell types.

To identify proteins in the MAVS pathway that might selectively control type I or type III interferon expression, we focused on the most downstream components of the interferon cascade: transcription factors. IFN-β is induced by the combined action of a complex of transcription factors termed the enhanceosome[21]. This involves IRF3 and IRF7, NF-κB and AP-1, the latter of which is activated by MAP kinases (MAPK). The *IFNL1* promoter contains binding sites for the transcription factors NF-κB and members of the interferon regulatory factor (IRF) family[21]. We used an siRNA-based approach to knock down IRF3 (**Supplementary Fig. 2d**)[32]. Consistent with the role of IRF3 as a critical regulator of antiviral immunity, depletion of IRF3 completely prevented the expression of both classes of interferon in response to SeV and DenV infection (**Fig. 3e**,**f**). siRNA-mediated knockdown of IRF7 marginally reduced both type I and III interferon induction to a similar extent (**Fig. 3g**), which suggested that this transcription factor has a limited role in the production of both cytokines. The *IFNL1* promoter also includes four NF-κB binding sites. To test the requirement for NF-κB in production of IFN-λ1, we used two small-molecule inhibitors, pyrrolidinedithiocarbamate ammonium (PDTC) and Bay11 (**Fig. 3h**,**i**). Either of these inhibitors blocked SeV-mediated production of *IFNL1* and *IFNB1* mRNA with comparable efficiency, which suggested that NF-κB is also required for the induction of IFN-λ1 in this system. Thus, several common regulatory factors exist that promote the expression of type I and type III interferon genes.

In addition to NF-κB and IRF proteins, the AP-1 transcription factor promotes the expression of IFN-β[21]. AP-1 is a large protein complex composed of dimers of members of the c-Jun, c-Fos and ATF families. These complexes are activated by MAPKs such as extracellular regulated kinase Erk, p38 or c-Jun N-terminal kinase Jnk. The role of AP-1 or MAPKs in production of type III interferons is unknown. We used small-molecule inhibitors of Jnk (SP600215), MEK and Erk (PD98059) or p38 (SB202190) on Huh7 hepatocytes to assess the role of each MAPK in interferon gene expression in response to SeV infection (**Fig. 4a**). Whereas p38, Jnk or MEK-Erk inhibition disrupted expression of *IFNB1* mRNA to varying extents, only p38 inhibitors disrupted expression of *IFNL1* mRNA (**Fig. 4a**). Treatment with Jnk or MEK-Erk inhibitors did not interfere with expression of type III interferons (**Fig. 4a**). siRNA-mediated knockdowns Erk family members confirmed their selective role in the expression of *IFNB1* mRNA (**Fig. 4b** and **Supplementary Fig. 2e**). Results obtained with siRNA-mediated knockdown of p38 differed from the results obtained with inhibitors, and suggested a selective role for this MAPK family in expression of IFN-β (**Fig. 4c** and **Supplementary Fig. 2f**). These data indicate that each component of the enhanceosome is necessary for expression of *IFNB1* but that a subset of enhanceosome components is sufficient for expression of *IFNL1* mRNA. Thus, it stands to reason that distinct signaling pathways may exist that selectively promote expression of type III interferon genes without activating expression of type I interferons.

The above data revealed that some MAPKs are selectively needed for the expression of type I interferons. To determine whether factors exist that are selectively needed for expression of type III interferons, we considered the transcription factor IRF1. Although IRF1 is encoded by an ISG, it is present in a variety of cells before viral

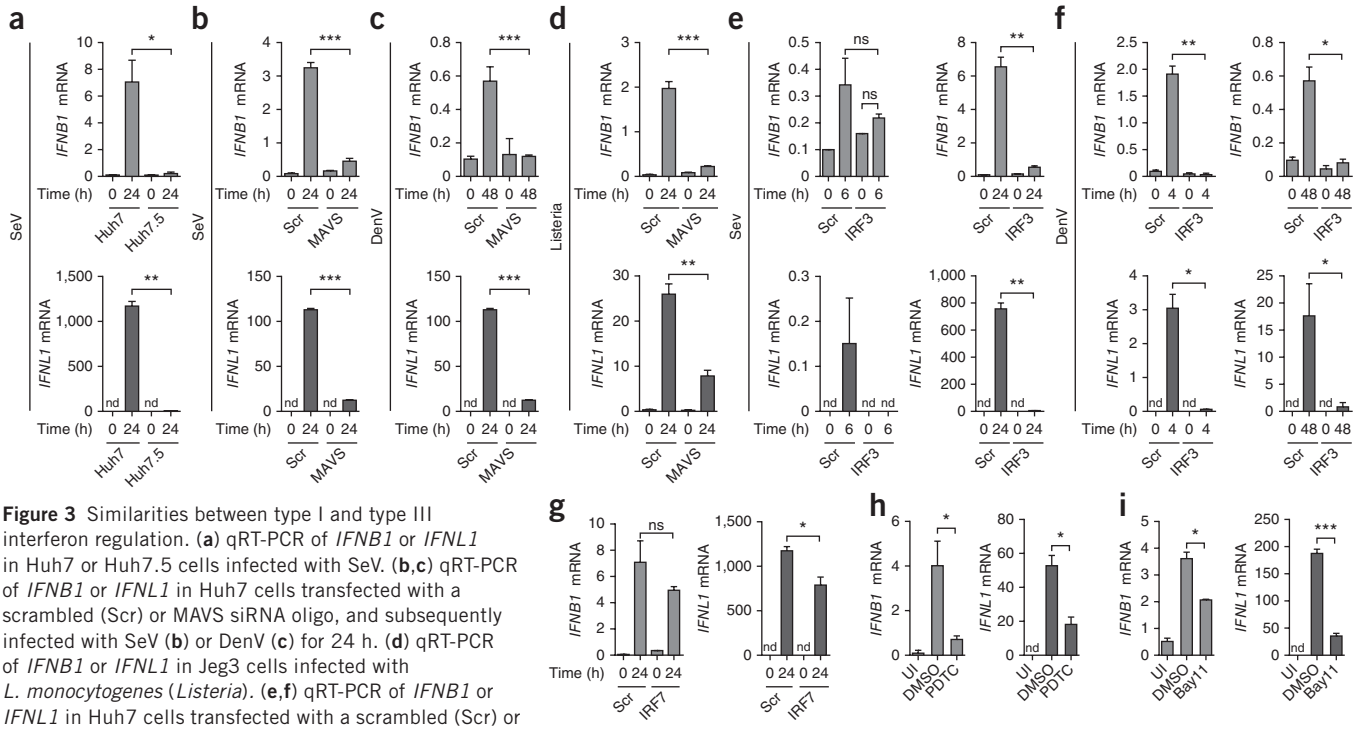

Figure 3 Similarities between type I and type III interferon regulation. (**a**) qRT-PCR of *IFNB1* or *IFNL1* in Huh7 or Huh7.5 cells infected with SeV. (**b**,**c**) qRT-PCR of *IFNB1* or *IFNL1* in Huh7 cells transfected with a scrambled (Scr) or MAVS siRNA oligo, and subsequently infected with SeV (**b**) or DenV (**c**) for 24 h. (**d**) qRT-PCR of *IFNB1* or *IFNL1* in Jeg3 cells infected with *L. monocytogenes* (*Listeria*). (**e**,**f**) qRT-PCR of *IFNB1* or *IFNL1* in Huh7 cells transfected with a scrambled (Scr) or IRF3 siRNA and infected with SeV (**e**) or DenV (**f**) for the durations indicated. (**g**) Experiment as in **e**, except cells were depleted of IRF7. (**h**,**i**) qRT-PCR of *IFNB1* or *IFNL1* in Huh7 cells treated with the NF-κB inhibitors PDTC (**h**) or Bay11 (**i**) and infected with SeV. UI, uninfected. Data are representative of three (**h**,**i**), four (**a**–**d**) or five (**e**–**g**) experiments (error bars, s.e.m.; $n = 3$ technical replicates). $^*P < 0.05$; $^{**}P < 0.01$; $^{***}P < 0.001$; ns, not significant (two-tailed Student's *t*-test). nd, not detected.

infection[33] (**Supplementary Fig. 2g**). IRF1 had been the first IRF family member shown to bind the *IFNB1* promoter[33], suggesting an important role in regulating expression of this gene. However, later IRF1 had been demonstrated to be dispensable for expression of type I interferons during viral infections of *Irf1*-deficient MEFs or mice[34]. IRF1 was also implicated in type I interferon–independent antiviral responses[2,35], perhaps via interactions with the *IFNL1* promoter in the lung[36,37]. We used siRNA-based approaches to define the role of IRF1 in the regulation of interferon expression. We carried out RNA interference–based knockdown of IRF1 in Huh7 cells (**Supplementary Fig. 2g**), which we subsequently infected with SeV. Knockdown of IRF1 had no effect on *IFNB1* mRNA levels 6 h after infection but completely inhibited expression of *IFNL1* mRNA after SeV infection (**Fig. 4d**). These data reveal an important role for IRF1 in controlling expression of type III interferons.

At late time points of infection (24 h), IRF1 knockdown reduced the production of both classes of interferons (**Fig. 4d**). However, at this late time point, the synergistic effects of secreted interferons and RLR signaling may complicate our ability to explain this observation. A useful means to address the role of IRF1 in interferon expression would be to study a virus that prevents signaling induced by secreted interferons. DenV is useful in this regard, as this virus blocks signaling downstream of interferon receptor ligation[38]. Although IRF1 was not required for expression of *IFNB1* in response to DenV, it promoted expression of *IFNL1* mRNA (**Fig. 4e**). As both IRF1 and IRF3 regulate *IFNL1* mRNA expression, we considered the possibility that IRF1 might somehow regulate the activation of IRF3. We assessed this by determining whether IRF3 can be phosphorylated in Huh7 cells that have been depleted of IRF1 through the use of siRNAs. We found that SeV infection induced the phosphorylation of IRF3 within 3 h of infection, even when IRF1 was knocked down (**Fig. 4f**). This result suggests that IRF1 and IRF3 are activated independently of each other but act together to promote expression of *IFNL1* mRNA. These data reveal an important role for IRF1 in the control of expression of type III interferons induced by multiple viral pathogens, especially during the primary phase of infection. Thus, IRF1 can be considered a counter to Erk, in that it is selectively required for expression of type III interferons, whereas Erk is selectively required for expression of type I interferons. Taken together, these data demonstrate that many common regulators control type I and type III interferon expression, but these genes can also be expressed independently of each other.

Peroxisomal MAVS induces selective expression of IFN-λ

We showed above that peroxisomal MAVS induces secretion of a factor that can cross species to activate a Jak-STAT pathway that is regulated by Jak2. We also showed that human type III interferon signaling is regulated by Jak2, but type I interferon signaling is not. These results suggest that peroxisomal MAVS preferentially induces type III interferons. To test this prediction directly, we needed a cell type that expresses high levels of type III interferons and expresses MAVS selectively on peroxisomes. Therefore we engineered Huh7 cells to stably express the relocalized MAVS transgenes[2] described above that encode either wild-type MAVS or variants that are localized specifically to mitochondria, peroxisomes or the cytosol. The resulting cell populations were sorted by flow cytometry to select clones that express comparable amounts of the transgenes (**Supplementary Fig. 2h**). Then we depleted the endogenous *MAVS* mRNA by using siRNAs that target the 5′ untranslated region of the *MAVS* mRNA, which resulted in cell lines that preferentially expressed the transgene of interest. To test whether peroxisomal MAVS in human cells could induce STAT1 phosphorylation in a Jak2-dependent manner, we treated cells with the pan-Jak inhibitor pyridone 6 and the Jak2 inhibitors AG490 and HBC. Infection with SeV induced phosphorylation of STAT1 in the cells expressing the wild-type MAVS,

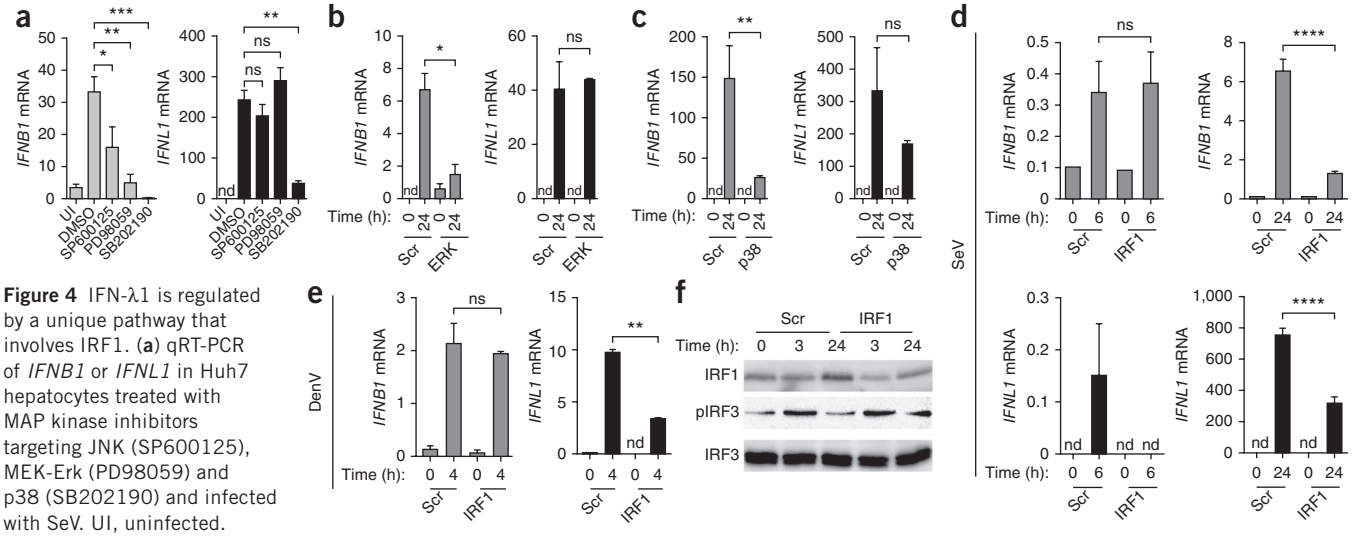

Figure 4 IFN-λ1 is regulated by a unique pathway that involves IRF1. (**a**) qRT-PCR of *IFNB1* or *IFNL1* in Huh7 hepatocytes treated with MAP kinase inhibitors targeting JNK (SP600125), MEK-Erk (PD98059) and p38 (SB202190) and infected with SeV. UI, uninfected. (**b**,**c**) qRT-PCR of *IFNB1* or *IFNL1* in Huh7 cells depleted of ERK (**b**) or p38 (**c**) or transfected with a scrambled (Scr) siRNA oligo, and infected overnight with SeV. (**d**,**e**) *IFNB1* or *IFNL1* qRT-PCR of Huh7 cells depleted of IRF1 and infected with SeV (**d**) or DenV (**e**) for the durations indicated. (**f**) Immunoblot analysis of IRF3 phosphorylation (pIRF3) with a phosphospecific antibody in Huh7 cells depleted of IRF1 or transfected with a Scr oligo and infected with SeV for 3 h and 24 h. Data are representative of two (**a**–**c**) or three (**d**–**f**) experiments (error bars, s.e.m.; $n = 3$ technical replicates). $^{*}P < 0.05$; $^{**}P < 0.01$; $^{***}P < 0.001$; $^{****}P < 0.0001$ (one-way ANOVA (**a**) or two-tailed Student's *t*-test (**b**–**e**)). ns, not significant; nd, not detected.

MAVS-pex or MAVS-mito (**Fig. 5a**). This response was blocked by all the inhibitors listed above, which indicated that MAVS-pex Huh7 cells respond similarly to MAVS-pex MEFs and can be used to test whether MAVS localized on peroxisomes induces expression of type III interferons. We noted that infection with SeV induced a weak phosphorylated STAT1 signal in cells with the allele encoding the signaling-deficient MAVS-cyto, probably resulting from incomplete knockdown of MAVS (**Fig. 5a**). This observation highlights some limitations of this system but also the importance of this negative control in subsequent experiments. Indeed, we found some residual SeV-mediated interferon production in cells expressing MAVS-cyto (**Fig. 5b**). Therefore, interferon levels produced by the MAVS-cyto line were considered to be the 'background' expression, above which signaling was considered significant (one-way ANOVA $P < 0.05$). In response to infection with SeV, only cells with alleles encoding wild-type MAVS and MAVS-mito induced expression of *IFNB1* mRNA, whereas MAVS-pex cells did not (**Fig. 5b**). However, MAVS-pex cells induced the expression of *IFNL1* mRNA (**Fig. 5b**). Infection with DenV (**Fig. 5c**,**d**) yielded comparable results: peroxisomal MAVS induced *IFNL1* but not *IFNB1* mRNA, whereas wild-type and mitochondrial MAVS induced both. The magnitude and kinetics of each transcriptional response differed greatly between viral infections, a result that likely reflects some aspect of the diverse lifecycles of the pathogens examined.

To determine whether the ability of peroxisomal MAVS to induce expression of type III interferon extended to bacterial infections, we returned to *L. monocytogenes* and Jeg3 cells, in which MAVS transgenes were overexpressed (**Supplementary Fig. 2i**). As infection with this bacterium disrupts mitochondria[39], and mitochondrial disruption hinders RLR signaling from this organelle[40], we hypothesized that peroxisomal MAVS might have a dominant role in the interferon response to *L. monocytogenes* infection. Indeed, in Jeg3 trophoblasts, where the interferon response to *L. monocytogenes* is MAVS-dependent (**Fig. 3d**), expression of peroxisomal MAVS strongly potentiated the ability of these cells to express *IFNL1*, although *IFNB1* mRNA was also induced (**Fig. 5e**). Overexpression of MAVS-mito did not induce the expression of any class of interferon above those induced by MAVS-cyto (**Fig. 5e**). The observation that peroxisomal MAVS contributes to type I interferon expression during *L. monocytogenes* infection, but not during viral infection, is noteworthy. One potential explanation for this finding is based on the fact that in addition to RLRs, *L. monocytogenes* activates other pattern recognition receptors in the cytosol[41]. The transcription factors activated by RLRs and other pattern recognition receptors may synergize to create a transcriptional profile distinct from that seen for viruses that only activate RLRs.

Although the above experiments revealed the ability of peroxisomal MAVS to induce the selective expression of type III interferons, the magnitude of interferon and ISG expression was less than that observed for cells expressing wild-type MAVS. This result is consistent with prior work showing that MAVS signaling from peroxisomes and mitochondria (coordinated around the mitochondria-associated membrane) synergize to induce maximal expression of antiviral genes[2,9]. To determine whether the amount of interferons released by cells expressing MAVS-pex was functional, we asked whether culture supernatants from infected cells could confer an antiviral state. We transferred culture supernatants from infected MAVS-pex Huh7 cells onto Huh7.5 cells and assessed the ability of VSV to replicate. In response to either SeV or DenV (**Fig. 5f**), peroxisomal MAVS induced the release of functional amounts of interferons that blocked VSV replication. These data establish peroxisomes as an organelle that can induce selective expression of type III interferons upon activation of the RLR-MAVS pathway.

To determine whether the pathway leading from peroxisomal MAVS was similar to that observed in wild-type cells, we assessed the effect of MAPK inhibitors on virus-induced gene expression. Whereas wild-type MAVS signaling was inhibited by inhibitors of Jnk (SP600125), MEK and Erk (PD98059) and p38 (SB202190), production of *viperin* mRNA in Huh7 cells expressing MAVS-pex was unaffected (**Fig. 5g**). siRNA-mediated knockdown of Erk in MEFs also abolished the ability of SeV to induce phosphorylation of STAT1 upon signaling by wild-type MAVS, but not MAVS-pex (**Fig. 5h** and **Supplementary Fig. 2j**), which confirmed that this MAPK does not control type III interferon responses.

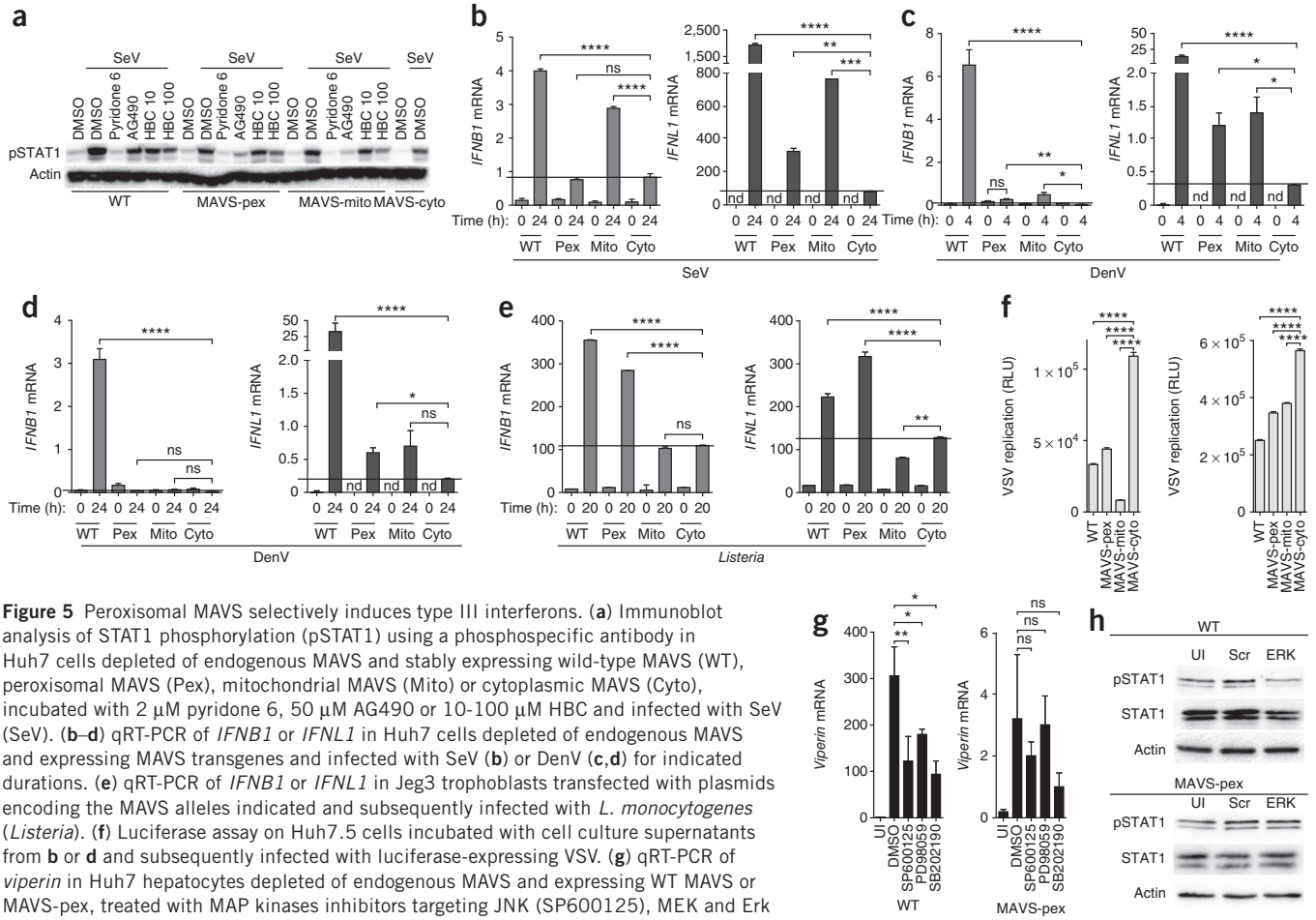

Figure 5 Peroxisomal MAVS selectively induces type III interferons. (**a**) Immunoblot analysis of STAT1 phosphorylation (pSTAT1) using a phosphospecific antibody in Huh7 cells depleted of endogenous MAVS and stably expressing wild-type MAVS (WT), peroxisomal MAVS (Pex), mitochondrial MAVS (Mito) or cytoplasmic MAVS (Cyto), incubated with 2 μM pyridone 6, 50 μM AG490 or 10-100 μM HBC and infected with SeV (SeV). (**b**–**d**) qRT-PCR of *IFNB1* or *IFNL1* in Huh7 cells depleted of endogenous MAVS and expressing MAVS transgenes and infected with SeV (**b**) or DenV (**c**,**d**) for indicated durations. (**e**) qRT-PCR of *IFNB1* or *IFNL1* in Jeg3 trophoblasts transfected with plasmids encoding the MAVS alleles indicated and subsequently infected with *L. monocytogenes* (*Listeria*). (**f**) Luciferase assay on Huh7.5 cells incubated with cell culture supernatants from **b** or **d** and subsequently infected with luciferase-expressing VSV. (**g**) qRT-PCR of *viperin* in Huh7 hepatocytes depleted of endogenous MAVS and expressing WT MAVS or MAVS-pex, treated with MAP kinases inhibitors targeting JNK (SP600125), MEK and Erk (PD98059) and p38 (SB202190). (**h**) Immunoblot analysis of STAT1 phosphorylation with a phosphospecific antibody in MAVS-depleted MEFs expressing WT MAVS (top) or MAVS-pex (bottom) infected with reovirus for 4 h. Data are representative of two (**g**), three (**a**,**h**), four (**c**–**f**) or five (**b**) experiments (error bars, s.e.m. (**b**–**e**) or s.d. (**f**,**g**); $n = 3$ technical replicates). $^{*}P < 0.05$; $^{**}P < 0.01$; $^{****}P < 0.0001$ (one-way ANOVA). ns, not significant; nd, not detected.

Peroxisome abundance controls the production of IFN-λ

Although the type I interferon system appears to be important in most mammalian cell types, the type III interferons appear to be most critical at mucosal surfaces, in particular in epithelial cells of the intestine, liver and lung. These observations suggest that epithelial cells might exhibit unusual cell biological characteristics that enhance the type III interferon system. To address this possibility, we turned our attention to human T84 intestinal epithelial cells, which can be differentiated into a polarized monolayer of cells that exhibit many functional and morphological properties of primary epithelia. Differentiation of T84 cells occurs over the course of several days, which allows us to determine whether the process of epithelial differentiation into a polarized monolayer would influence the RLR-MAVS pathway. As expected, the transepithelial resistance of the T84 cell monolayer increased over time, which is a functional indication of epithelial polarization (**Fig. 6a**). As T84 intestinal epithelial cells polarized, the abundance of peroxisomes increased, whereas that of mitochondria remained unchanged (**Fig. 6b** and **Supplementary Fig. 3**). This increase in abundance of peroxisomes correlated with an increase in expression of the gene encoding Pex11β (*PEX11B*), which is a master regulator of peroxisome proliferation (**Fig. 6c**). To determine whether the change in the abundance of peroxisomes relative to that of mitochondria influences RLR-MAVS signaling events, we infected the T84 cells with the intestinal pathogen reovirus at various times during the differentiation process. At any day of differentiation, the T84 cells responded equally well to reovirus and produced roughly equal amounts of *IFNB1* mRNA (**Fig. 6d**). In contrast, the magnitude of the IFN-λ response (*IFNL1* mRNA levels) increased over time (**Fig. 6d**,**e**), which correlated with an increase in *PEX11B* mRNA, peroxisome abundance and transepithelial resistance. These data reveal that as epithelial cells differentiate into a polarized monolayer, they shift from a dominant type I interferon to type III interferon response, which may be caused by an increase in peroxisome abundance.

To determine whether increasing abundance of peroxisomes was sufficient to influence the RLR-MAVS pathways, we induced the proliferation of peroxisomes in Huh7 cells by overexpression of Pex11β. As expected[42], we observed a marked increase of Pex14-positive peroxisomes in Pex11β-expressing cells (**Fig. 6f**). This increase in the abundance of peroxisomes correlated with an increase in production of *IFNL1* mRNA in response to SeV infection, but expression of *IFNB1* mRNA was unaffected (**Fig. 6g**). These data therefore provide a direct link between the abundance of peroxisomes and the quality of the interferon response induced by the RLR-MAVS pathway.

Finally, we determined whether the endogenous MAVS protein on peroxisomes was sufficient to induce type III interferons. Disruption of mitochondrial function with the protonophore carbonyl cyanide m-chlorophenylhydrazone (CCCP) has been used to reveal the importance of mitochondrial integrity for RLR signaling[40]. Notably,

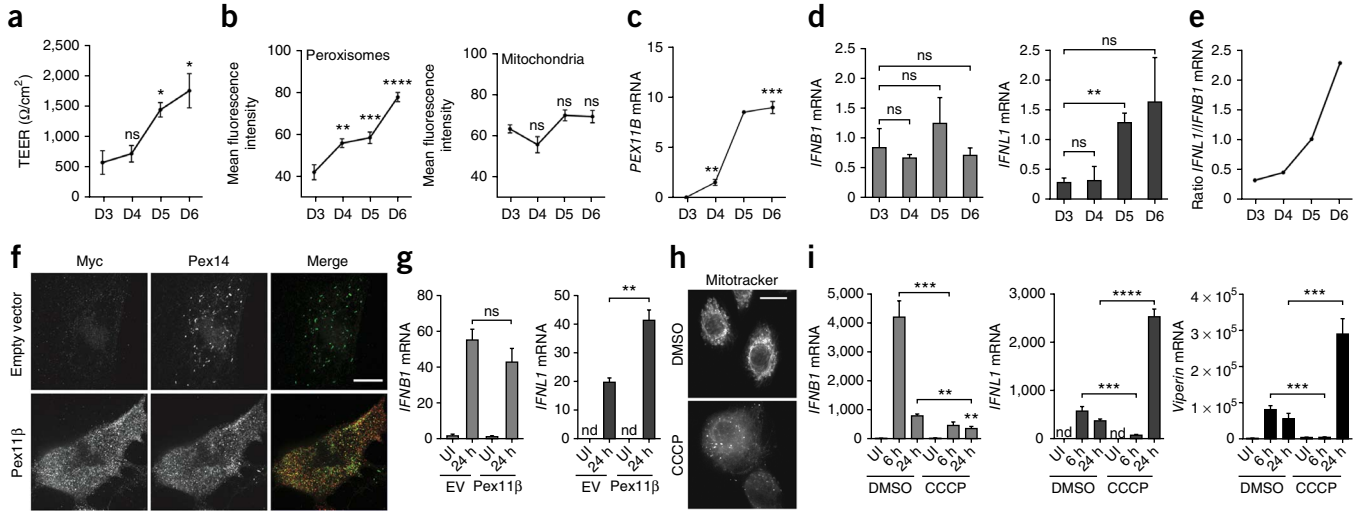

Figure 6 The abundance and function of mitochondria and peroxisomes affects the quality of the interferon response. (**a**) Transepithelial electrical resistance (TEER) of T84 colonic epithelial polarizing on transwells measured between day 3 and day 6 after plating (D3–D6). (**b**) Densitometric analyses of multiple images of peroxisome (left) and mitochondria (right) in polarizing T84 cells. (**c**) qRT-PCR of *PEX11B* in polarizing T84 cells at the time points indicated. Unless otherwise indicated, comparisons were made between day 3 (D3) samples and others (**a**–**c**). (**d**) qRT-PCR of *IFNB1* or *IFNL1* in T84 cells infected every day for 24 h with reovirus. (**e**) Ratio of *IFNL1* to *IFNB1* mRNA induced by reovirus infection over time. (**f**) Confocal microscopy analysis of Pex14-labelled Huh7 hepatocytes expressing the peroxisome biogenesis regulator Pex11β. Scale bar, 10 μM. (**g**) qRT-PCR of *IFNB1* or *IFNL1* in Pex11β-expressing cells or control (empty vector, EV) infected with SeV for 24 h. UI, uninfected. (**h**) Confocal microscopy analysis of mitotracker-stained keratinocytes treated with DMSO or the mitochondria membrane potential–disrupting agent CCCP. Scale bar, 10 μM. (**i**) qRT-PCR of *IFNB1* or *IFNL1* in CCCP-treated keratinocytes infected with SeV for the indicated durations. Data are a summary of four experiments (**a**) or are representative of three experiments (**b**–**i**; over 500 cells were inspected as shown in **f**,**h**); error bars, s.e.m.; $n = 4$ experiments (**a**), $n = 60$ fields of view (**b**) or $n = 3$ technical replicates (**c**–**e**,**g**,**i**). $^*P < 0.05$; $^{**}P < 0.01$; $^{***}P < 0.0001$ (one-way ANOVA). ns, not significant; nd, not detected.

peroxisome functions are unaffected by CCCP[43]. We reasoned that if endogenous peroxisome-localized MAVS functioned to control expression of type III interferons, then CCCP-treated cells may retain the ability to induce these interferons. Alternatively, if mitochondria are the sole subcellular site of RLR-MAVS signaling, then treatment with CCCP should block expression of all RLR-induced genes to a similar extent. To address this possibility, we used primary human keratinocytes because they produce and respond to type III interferons and because they tolerate treatment with CCCP. Over the course of the 3-d experiments, keratinocytes remained viable and robust. Treatment with CCCP eradicated the functional mitochondrial pool in these cells, as assessed by mitotracker staining (**Fig. 6h**). Under these conditions, SeV-mediated production of *IFNB1* mRNA was completely inhibited (**Fig. 6i**), similar to what has been observed[40]. By contrast, expression of the ISG *viperin* and *IFNL1* was enhanced in the presence of CCCP (**Fig. 6i**). These data indicate that even in primary cells, the endogenous RLR signaling pathway can operate in the absence of functional mitochondria, and that this pathway can be 'rewired' to produce only type III interferons, likely from peroxisomes.

'Zellweger cells' implicate peroxisomes in RLR signaling

The studies described above suggested that RLR signaling via MAVS can occur in cells lacking functional mitochondria, thus raising the question of how MAVS populates peroxisomes and how these organelles are functionally interconnected. To address these questions, we used cells derived from human patients with Zellweger syndrome, which is a peroxisome biogenesis disorder. These patients have defective peroxisomes and suffer from various developmental abnormalities, which often results in death early in life[44]. Death can be associated with infection (usually pneumonia) and patients display elevated cytokine levels, particularly in the brain[45]. The immunological basis for these observations is unclear, as cells from patients with Zellweger disease (here referred to as 'Zellweger cells') have not been thoroughly examined for alterations in innate immune signaling pathways.

Zellweger cells that lack a functional *PEX14* gene contain peroxisomal membranes that stain for the membrane protein PMP70, but these organelles lack all cargo that is normally present in the lumen, such as catalase[44] (**Supplementary Fig. 4**). We found that cells lacking Pex14 retain MAVS on their limiting membrane (**Supplementary Fig. 5**), suggesting that MAVS does not require Pex14 for its ability to localize to peroxisomes. Thus, MAVS can be categorized as a peroxisomal membrane protein that is targeted to these organelles by Pex14-independent means.

Unlike in the case with Pex14 deficiency, patients with Zellweger disease that lack functional Pex16 or Pex19 lack physically distinct peroxisomes[46] (**Supplementary Fig. 4**). In these cells, peroxisomal membrane proteins can be mistargeted to mitochondria[47,48]. Thus, Pex19-deficient or Pex16-deficient cells contain mitochondria that display both peroxisomal and mitochondrial proteins on their limiting membranes. These observations are intriguing when considering recent work which suggests that physical interactions between mitochondria and peroxisomes lead to an enhanced RLR-dependent response to viral infection[9]. Although the molecular basis for these observations remains unclear, it seems reasonable that membrane proteins on each organelle would interact to promote more efficient MAVS-dependent cellular responses. For this reason, we wondered if Zellweger cells lacking Pex19, which contain peroxisomal and mitochondrial proteins on the same organelle, might display an aberrant response to viral infection. To address this possibility, we infected Pex19-deficient cells or Pex19-deficient cells stably expressing Pex19 with mammalian reovirus. Then we examined the cells 9 h and 16 h after infection by microarray analysis. Reovirus infection of both genotypes induces a gene expression profile typical for an antiviral

immune response, as apparent from Gene Ontology term analysis (**Supplementary Fig. 6a**). Global transcriptome analysis revealed that Pex19-deficient cells displayed a higher antiviral response at all time points examined (**Supplementary Fig. 6b–d**). Of note, of the 20 genes that are most highly upregulated in Pex19-deficient cells compared to reconstituted cells, most are ISGs (**Supplementary Fig. 6d**). These data suggest that the presence of mitochondria containing peroxisomal proteins promotes greater RLR-dependent responses. These studies underscore the important role of peroxisomes in regulating RLR signaling, and provide to our knowledge the first insight into immunological consequences of Pex19 deficiency in human disease.

DISCUSSION

We demonstrated that RLRs can signal via MAVS from peroxisomes to drive the synthesis of type III interferons. We revealed that the RLR pathway can induce expression of different classes of interferon genes and that the decision of which genes to induce is determined by the location in the cell where RLR signaling is initiated. Our results therefore highlight how the microenvironments of different cell types can influence the activity of a given signaling pathway. First, using both direct (mRNA quantification) and indirect (functional assays) approaches, we found that the RLR network can induce the expression of type I and type III interferons in response to infections with diverse intracellular pathogens, in seven primary human cell types and three different cell lines. Second, the ability of type III interferons to be expressed was directly controlled by the differentiation state of intestinal epithelial cells and occured as a function of the abundance of peroxisomes. Third, depletion of mitochondria in primary human keratinocytes did not inactivate the RLR pathway but shifted the RLR pathway to be a primary producer of type III interferons. These data identify type III interferons as a major component of the RLR pathway emanating from peroxisomes and suggest that cell type–specific expression of classes of interferons can be achieved by altering the abundance of peroxisomes or mitochondria in a given cell population.

It has been generally considered that expression of type I and type III interferons is coregulated and induced by a common (unknown) signaling pathway. Our work to define the means by which peroxisomal MAVS can induce antiviral gene expression revealed that these interferon classes can be induced differentially. We identified the existence of complementary but distinct regulators that control expression of type I and type III interferons. We found that the transcription factor IRF1 is necessary for expression of type III interferons and Erk MAPKs are necessary for expression of type I interferons. These data suggest a plausible model whereby expression of type III interferons from peroxisomes can be achieved without the expression of type I interferons. We suggest that the MAVS pathway from peroxisomes does not activate Erk, but does activate NF-κB and IRF3. This partial activation of the components of the classically defined enhanceosome would preclude expression of *IFNB1* but would permit the expression of *IFNL1*. When considered in this context, it would be expected that pathogens that activate multiple pattern recognition receptors may create a means of 'complementing' the defect in MAPK signaling and allow the peroxisomal pathway to induce expression of type I interferons. This idea may therefore explain why peroxisomal MAVS induces the expression of type I and type III interferons during *Listeria* infections, as these bacteria also strongly activate MAPK family members.

Although our studies highlight how type III interferons can be induced selectively from peroxisomes in epithelial cells, they also raise the question of why these different interferon families exist. One would expect that type III interferons would induce different cellular responses than their type I counterparts. However, analysis of gene expression indicated a largely overlapping set of genes that are induced by the type I and type III interferon receptors. Why then is the expression of the type III interferon receptor selectively detected on mucosal epithelial cells, and why is the ability of intestinal epithelia to express type III interferons dependent on the degree of cell polarization? We propose that in addition to transcriptional responses, the RLR pathway (via type III interferons) may elicit cellular responses that are more compatible with the specific homeostatic functions of epithelia than RLR-induced type I interferons. Possible examples of such cellular responses include activities that may influence cell-cell communication, viability or metabolism. This prediction may explain why type III interferon expression is linked to the polarization of T84 intestinal epithelial cells, and may explain the benefit of allowing RLR signaling to occur from multiple organelles. By separating the subcellular sites of RLR signaling and allowing different cellular responses to occur from these different sites, the RLR network can be modified to emphasize or deemphasize an organelle-specific response to fit the homeostatic needs of any given type of cell. The findings presented in this study support these ideas and provide a mandate for future work on the cell type–specific functions of the innate immune signaling networks in mammals.

METHODS

Methods and any associated references are available in the online version of the paper.

Accession codes. Gene Expression Omnibus: GSE56783.

Note: Any Supplementary Information and Source Data files are available in the online version of the paper.

ACKNOWLEDGMENTS

We thank members of the Kagan laboratory for helpful discussions, M. Fransen (Katholieke Universiteit, Leuven, Belgium) for providing cell lines and reagents, and B. Nelms for bioinformatic assistance. Microarray analyses were performed by members of the Molecular Genetics Core Facility at Boston Children's Hospital. J.C.K. is supported by US National Institutes of Health grants AI093589, AI072955 and P30 DK34854, and an unrestricted gift from Mead Johnson & Company. J.C.K. received an Investigators in the Pathogenesis of Infectious Disease Award from the Burroughs Wellcome Fund. C.O. is supported by a fellowship from the Crohn's and Colitis Foundation of America. F.S. is funded by the Agence National de la Recherche (ANR project Mitopatho). E.D. is supported by an Erwin Schrödinger Fellowship of the Austrian Science Fund (FWF). K.M.F. is supported through the Herchel Smith Graduate Fellowship Program. L.G. and J.C.K. are supported by a Massachusetts Institute of Technology–Boston Children's Hospital Collaborative grant. L.G. is supported by US National Institutes of Health grant CA159132. P.C. is supported by European Research Council Advanced Grant 233348 MODELIST and by Howard Hughes Medical Institute as a senior international research scholar.

AUTHOR CONTRIBUTIONS

C.O., E.D., A.F.D. and K.M.F. did and analyzed all experiments involving viral infections and peroxisome or mitochondria cell biology; F.S., H.B. and P.C. performed and analyzed all *L. monocytogenes* infection experiments. S.B. prepared and analyzed reovirus stocks. A.F.D. and L.G. prepared and analyzed DenV stocks. C.O. and J.C.K. wrote the manuscript. All authors edited the manuscript.

COMPETING FINANCIAL INTERESTS

The authors declare no competing financial interests.

1. Takeuchi, O. & Akira, S. Innate immunity to virus infection. *Immunol. Rev.* **227**, 75–86 (2009).
2. Dixit, E. *et al.* Peroxisomes are signaling platforms for antiviral innate immunity. *Cell* **141**, 668–681 (2010).

3. Noyce, R.S., Collins, S.E. & Mossman, K.L. Identification of a novel pathway essential for the immediate-early, interferon-independent antiviral response to enveloped virions. *J. Virol.* **80**, 226–235 (2006).
4. Noyce, R.S. *et al.* Membrane perturbation elicits an IRF3-dependent, interferon-independent antiviral response. *J. Virol.* **85**, 10926–10931 (2011).
5. Peltier, D.C., Lazear, H.M., Farmer, J.R., Diamond, M.S. & Miller, D.J. Neurotropic arboviruses induce interferon regulatory factor 3-mediated neuronal responses that are cytoprotective, interferon independent, and inhibited by Western equine encephalitis virus capsid. *J. Virol.* **87**, 1821–1833 (2013).
6. Nakhaei, P., Genin, P., Civas, A. & Hiscott, J. RIG-I-like receptors: sensing and responding to RNA virus infection. *Semin. Immunol.* **21**, 215–222 (2009).
7. Kato, H. *et al.* Differential roles of MDA5 and RIG-I helicases in the recognition of RNA viruses. *Nature* **441**, 101–105 (2006).
8. Seth, R.B., Sun, L., Ea, C.K. & Chen, Z.J. Identification and characterization of MAVS, a mitochondrial antiviral signaling protein that activates NF-kappaB and IRF 3. *Cell* **122**, 669–682 (2005).
9. Horner, S.M., Liu, H.M., Park, H.S., Briley, J. & Gale, M. Jr. Mitochondrial-associated endoplasmic reticulum membranes (MAM) form innate immune synapses and are targeted by hepatitis C virus. *Proc. Natl. Acad. Sci. USA* **108**, 14590–14595 (2011).
10. Belgnaoui, S.M., Paz, S. & Hiscott, J. Orchestrating the interferon antiviral response through the mitochondrial antiviral signaling (MAVS) adapter. *Curr. Opin. Immunol.* **23**, 564–572 (2011).
11. Kotenko, S.V. IFN-lambdas. *Curr. Opin. Immunol.* **23**, 583–590 (2011).
12. Sumpter, R. Jr. *et al.* Regulating intracellular antiviral defense and permissiveness to hepatitis C virus RNA replication through a cellular RNA helicase, RIG-I. *J. Virol.* **79**, 2689–2699 (2005).
13. Frank, D.A., Mahajan, S. & Ritz, J. Fludarabine-induced immunosuppression is associated with inhibition of STAT1 signaling. *Nat. Med.* **5**, 444–447 (1999).
14. Stark, G.R. & Darnell, J.E. Jr. The JAK-STAT pathway at twenty. *Immunity* **36**, 503–514 (2012).
15. Meydan, N. *et al.* Inhibition of acute lymphoblastic leukaemia by a Jak-2 inhibitor. *Nature* **379**, 645–648 (1996).
16. Sandberg, E.M. *et al.* Identification of 1,2,3,4,5,6-hexabromocyclohexane as a small molecule inhibitor of jak2 tyrosine kinase autophosphorylation. *J. Med. Chem.* **48**, 2526–2533 (2005).
17. Veomett, M.J. & Veomett, G.E. Species specificity of interferon action: maintenance and establishment of the antiviral state in the presence of a heterospecific nucleus. *J. Virol.* **31**, 785–794 (1979).
18. Watling, D. *et al.* Complementation by the protein tyrosine kinase JAK2 of a mutant cell line defective in the interferon-gamma signal transduction pathway. *Nature* **366**, 166–170 (1993).
19. Berger Rentsch, M. & Zimmer, G. A vesicular stomatitis virus replicon-based bioassay for the rapid and sensitive determination of multi-species type I interferon. *PLoS One* **6**, e25858 (2011).
20. Lee, S.J., Kim, W.J. & Moon, S.K. Role of the p38 MAPK signaling pathway in mediating interleukin-28A-induced migration of UMUC-3 cells. *Int. J. Mol. Med.* **30**, 945–952 (2012).
21. Iversen, M.B. & Paludan, S.R. Mechanisms of type III interferon expression. *J. Interferon Cytokine Res.* **30**, 573–578 (2010).
22. Onoguchi, K. *et al.* Viral infections activate types I and III interferon genes through a common mechanism. *J. Biol. Chem.* **282**, 7576–7581 (2007).
23. Osterlund, P.I., Pietila, T.E., Veckman, V., Kotenko, S.V. & Julkunen, I. IFN regulatory factor family members differentially regulate the expression of type III IFN (IFN-lambda) genes. *J. Immunol.* **179**, 3434–3442 (2007).
24. Lasfar, A. *et al.* Characterization of the mouse IFN-lambda ligand-receptor system: IFN-lambdas exhibit antitumor activity against B16 melanoma. *Cancer Res.* **66**, 4468–4477 (2006).
25. Hermant, P. *et al.* Human but not mouse hepatocytes respond to interferon-lambda *in vivo*. *PLoS One* **9**, e87906 (2014).
26. Marukian, S. *et al.* Hepatitis C virus induces interferon-lambda and interferon-stimulated genes in primary liver cultures. *Hepatology* **54**, 1913–1923 (2011).
27. Sommereyns, C., Paul, S., Staeheli, P. & Michiels, T. IFN-lambda (IFN-lambda) is expressed in a tissue-dependent fashion and primarily acts on epithelial cells *in vivo*. *PLoS Pathog.* **4**, e1000017 (2008).
28. Pott, J. *et al.* IFN-lambda determines the intestinal epithelial antiviral host defense. *Proc. Natl. Acad. Sci. USA* **108**, 7944–7949 (2011).
29. de Macedo, F.C. *et al.* Histologic, viral, and molecular correlates of dengue fever infection of the liver using highly sensitive immunohistochemistry. *Diagn. Mol. Pathol.* **15**, 223–228 (2006).
30. Bierne, H. *et al.* Activation of type III interferon genes by pathogenic bacteria in infected epithelial cells and mouse placenta. *PLoS One* **7**, e39080 (2012).
31. Lebreton, A. *et al.* A bacterial protein targets the BAHD1 chromatin complex to stimulate type III interferon response. *Science* **331**, 1319–1321 (2011).
32. Tamura, T., Yanai, H., Savitsky, D. & Taniguchi, T. The IRF family transcription factors in immunity and oncogenesis. *Annu. Rev. Immunol.* **26**, 535–584 (2008).
33. Miyamoto, M. *et al.* Regulated expression of a gene encoding a nuclear factor, IRF-1, that specifically binds to IFN-beta gene regulatory elements. *Cell* **54**, 903–913 (1988).
34. Reis, L.F., Ruffner, H., Stark, G., Aguet, M. & Weissmann, C. Mice devoid of interferon regulatory factor 1 (IRF-1) show normal expression of type I interferon genes. *EMBO J.* **13**, 4798–4806 (1994).
35. Stirnweiss, A. *et al.* IFN regulatory factor-1 bypasses IFN-mediated antiviral effects through viperin gene induction. *J. Immunol.* **184**, 5179–5185 (2010).
36. Siegel, R., Eskdale, J. & Gallagher, G. Regulation of IFN-lambda1 promoter activity (IFN-lambda1/IL-29) in human airway epithelial cells. *J. Immunol.* **187**, 5636–5644 (2011).
37. Ueki, I.F. *et al.* Respiratory virus-induced EGFR activation suppresses IRF1-dependent interferon lambda and antiviral defense in airway epithelium. *J. Exp. Med.* **210**, 1929–1936 (2013).
38. Morrison, J., Aguirre, S. & Fernandez-Sesma, A. Innate immunity evasion by Dengue virus. *Viruses* **4**, 397–413 (2012).
39. Stavru, F., Bouillaud, F., Sartori, A., Ricquier, D. & Cossart, P. Listeria monocytogenes transiently alters mitochondrial dynamics during infection. *Proc. Natl. Acad. Sci. USA* **108**, 3612–3617 (2011).
40. Koshiba, T., Yasukawa, K., Yanagi, Y. & Kawabata, S. Mitochondrial membrane potential is required for MAVS-mediated antiviral signaling. *Sci. Signal.* **4**, ra7 (2011).
41. Stavru, F., Archambaud, C. & Cossart, P. Cell biology and immunology of Listeria monocytogenes infections: novel insights. *Immunol. Rev.* **240**, 160–184 (2011).
42. Schrader, M. *et al.* Expression of PEX11beta mediates peroxisome proliferation in the absence of extracellular stimuli. *J. Biol. Chem.* **273**, 29607–29614 (1998).
43. Narendra, D., Tanaka, A., Suen, D.F. & Youle, R.J. Parkin is recruited selectively to impaired mitochondria and promotes their autophagy. *J. Cell Biol.* **183**, 795–803 (2008).
44. Steinberg, S.J., Raymond, G.V., Braverman, N.E. & Moser, A.B. Peroxisome biogenesis disorders, Zellweger syndrome spectrum. in *GeneReviews* (eds., Pagon, R.A., Bird, T.D., Dolan, C.R., Stephens, K. and Adam, M.P.) (2003).
45. Eichler, F. & Van Haren, K. Immune response in leukodystrophies. *Pediatr. Neurol.* **37**, 235–244 (2007).
46. Waterham, H.R. & Wanders, R.J. Metabolic functions and biogenesis of peroxisomes in health and disease. *Biochim. Biophys. Acta* **1822**, 1325 (2012).
47. Halbach, A. *et al.* Targeting of the tail-anchored peroxisomal membrane proteins PEX26 and PEX15 occurs through C-terminal PEX19-binding sites. *J. Cell Sci.* **119**, 2508–2517 (2006).
48. Sacksteder, K.A. *et al.* PEX19 binds multiple peroxisomal membrane proteins, is predominantly cytoplasmic, and is required for peroxisome membrane synthesis. *J. Cell Biol.* **148**, 931–944 (2000).

ONLINE METHODS

Plasmids, antibodies, small interfering RNAs and recombinant proteins. Chimeric *MAVS* alleles were described[2]. Vector encoding MYC-PEX11B was obtained from M. Fransen (Katholieke Universiteit, Leuven, Belgium; ref. 42). Anti-viperin, MAVS, phospho STAT1, GFP, PMP70, catalase, mitochondrial HSP70, tubulin and actin antibodies were obtained from BioLegend (97736), Bethyl labs (A300-782A), BD Transduction (612132, Clone 14/P-STAT1), Clontech (632380) or Invitrogen (11122), Sigma (SAB4200181), Santa Cruz (sc-34280), Thermo (MA3-028, clone JG1), Sigma (T6074) and Sigma (A5441, clone AC-15), respectively. Antibodies to STAT1, phospho IRF3, phospho Jak2, Jak2 and IRF1 were obtained from BD Transductions (610115, clone 1/Stat1), Cell Signaling (4947), Santa Cruz (sc16566), Santa Cruz (sc278, clone HR-758) and Cell Signaling (8478, clone D5E4), respectively. Anti-Pex14 was obtained from M. Fransen. Taking advantage of the high concentration of biotin-dependent carboxylases in mitochondria, streptavidin–Alexa Fluor 488 was used to label mitochondria[49]. siRNAs to transcripts encoding IRF1 and IRF3 were obtained from Ambion with the respective sequences CCAGUGAUCUGUACAACU and ACAUAAAAUCUACGAGUU. siRNAs targeting *MAVS* and *IRF7* in Huh7 cells were obtained from Qiagen with the following sequences AACGACUUCUGUUCUGGAUAU and CCCGAGCTGACGTTCCTATA. siRNA targeting *MAVS* in Jeg3 cells (CCGUUUGCUGAAGACAAGA) was obtained from MWG Operon. siRNAs to sequences encoding mouse Jak1 (TACCAGGATGCGAATAAATAA), mouse Jak2 (ATGATTGGCAATGATAAACAA), human Erk1 (CCGGC CCATCTTCCCTGGCAA), human Erk2 (AACAAAGTTCGAGTAGCTATC) were obtained from Qiagen. siRNAs to sequences encoding human Erk1 (ID 77117) and Erk2 (ID 77106), and mouse STAT1 (ID 74445) were obtained from Ambion. siRNA to sequence encoding human p38 was obtained from Cell Signaling (6564).

Cell lines, retroviral gene transfer and transfections. MEFs, Huh7 and Jeg3 cells were cultured using to standard techniques. 293T ISRE Luciferase cells were obtained from N. Hacohen (Harvard University). T84 epithelial cells were cultured and polarized as previously described[50]. Primary human foreskin keratinocytes were a gift from K. Munger (Harvard Medical School) and were isolated from tissue from circumcisions of anonymous newborns and cultured as previously described[51]. Primary human hepatocytes and bronchial epithelial cells were obtained from Lonza and cultured according the manufacturer's recommendations. Primary myoblasts were obtained from Mytogen and cultured and infected as described[52]. Blood of healthy individuals was collected, and PBMCs were isolated using Lympholyte and SepMate columns or Ficoll gradient. Monocytes were purified using EasySep beads (StemCell Technologies). Pex14-deficient and Pex16-deficient human skin fibroblasts were obtained from M. Fransen. Pex19-deficient and reconstituted human skin fibroblasts as well as MEFs expressing chimeric *MAVS* alleles have been described[2]. The same chimeric MAVS alleles were introduced in Huh7 cells and then sorted for equal GFP fluorescence to normalize MAVS expression levels. Where indicated, Huh7 cells were transfected with 40 nM siRNA oligos using JetPRIME (Polyplus transfections) for 48 h. Knockdown in Jeg3 cells was carried out with 30 nM siRNA using Lipofectamine RNAiMAX (Invitrogen). Protein knockdown was determined by immunoblotting using standard techniques or real-time quantitative PCR (qRT-PCR), as described below. Transient DNA transfections in Jeg3 cells were carried out with 0.5 μg DNA/cm^3 using Fugene HD (Promega), following the manufacturer's recommendations.

Virus stocks, bacterial strains and infections. Reovirus type 3 Dearing Cashdollar was propagated in L929 cells and plaque-purified as described[53]. SeV was obtained from Charles River Labs. Dengue 2 virus strain New Guinea C was isolated from a febrile patient in the 1940s[54], and was propagated on C6-36 mosquito cells cultured in RPMI (Gibco) at 28 °C, 5% CO_2. Infectious C6-36 supernatant was titered by flow cytometry[55]. *L. monocytogenes* EGD strain (BUG600) has been described previously[56]. Cells were seeded 16–24 h before infection or transfection. On the day of the infection, medium was replaced with serum-free medium containing virions at multiplicities of infection (MOI) of 1 (DenV) or 100 (Reo) or 50 HAU/ml (SeV). *Listeria monocytogenes* infections were carried out at MOI of 0.1, as described[31].

Inhibitors and microscopy. With exception of fludarabine (Tocris Biosciences) and CCCP (Sigma), all inhibitors were from Calbiochem. Cells were incubated with 10–50 μM fludarabine, 2 μM pyridone 6, 10–50 μM AG490, 10–100 μM 1,2,3,4,5,6-hexabromocyclohexane (Jak2 inhibitor II, HBC), 5 μM Bay11, 50 μM PDTC, 30 μM PD98059, 100 μM SP600125, 10 μM SB202190 for 30 min, before infection or treatment. In case of interferon treatment, cells were incubated in fresh medium with 0.01 μg/ml human IFN-λ1 or mouse IFN-λ2 (Peprotech), 10 U/ml human IFN-β or 50 U/ml mouse IFN-β (PFL Interferon Source) for 2–5 h. Keratinocytes were incubated in media containing either 10 μM CCCP or DMSO. Cells were incubated for 48 h and then infected or incubated with 250 nM MitoTracker Deep Red FM (Molecular Probes) for 30 min at 37 °C before fixation in 2% paraformaldehyde in PBS. Confocal images were acquired using a spinning disk confocal head (CSU-X1, Perkin Elmer Co.) coupled to a fully motorized inverted Zeiss Axiovert 200M microscope equipped with a 63× lens (Pan Apochromat, 1.4 numerical aperture (NA)). The imaging system operates under control of SlideBook 5 (Intelligent Imaging Innovations Inc). Micrographs were processed with Adobe Photoshop.

mRNA detection, nCounter analysis and gene arrays. Cells were lysed in RLT buffer (Qiagen) supplemented with β-mercaptoethanol and passed through Qiashredder columns (Qiagen). RNA was then isolated using RNeasy columns (Qiagen) following the manufacturer's recommendations. RT-qPCR was carried out with a Bio-Rad iQ5 or CFX384 real-time cycler with Taqman probes as directed by the manufacturer. nCounter CodeSets were constructed to detect genes selected by the Gene-Selector algorithm and additional controls as described[57]. Purified RNA was hybridized for 16 h with the CodeSet and loaded onto the nCounter prep station, followed by quantification with the nCounter Digital Analyzer. To allow for side-by-side comparisons of nCounter experiments, we normalized the nCounter data in two steps. We first controlled for small variations in the efficiency of processing by normalizing measurements from all samples analyzed on a given run to the levels of chosen positive controls provided by the nCounter instrument. Second, we normalized the data obtained for each sample to the expression of a control gene (*GAPDH*). These genes have been described to be unchanged in cells exposed to a variety of infectious conditions[57]. For every sample, we computed the weighted average of the mRNA counts of the control transcript and normalized the sample's values by multiplying each transcript count by the weighted average of the controls.

Microarrays were performed by the Molecular Genetics Core Facility at Boston Children's Hospital supported by US National Institutes of Health grants P50-NS40828 and P30-HD18655. Quantile normalization was used for signal extraction and normalization. For comparison of gene expression profiles between genotypes and time points log-transformed data were plotted and a weighted linear fit calculated. For Gene Ontology analysis, *P* values were calculated using the hypergeometric distribution and adjusted for multiple hypotheses testing by Holm's method.

Statistics. GraphPad Prism was used for all statistical analyses. Statistical analysis was carried out by one-way analysis of variance (ANOVA) followed by Dunnett's test or unpaired Student's *t*-test (two-tailed). $P < 0.05$ was considered statistically significant. No pre-experiment statistical methods, randomization or blinding were used. Sample-size choice and assumption of normality were based on similar analyses in published studies.

49. Hollinshead, M., Sanderson, J. & Vaux, D.J. Anti-biotin antibodies offer superior organelle-specific labeling of mitochondria over avidin or streptavidin. *J. Histochem. Cytochem.* **45**, 1053–1057 (1997).
50. Lencer, W.I., Delp, C., Neutra, M.R. & Madara, J.L. Mechanism of cholera toxin action on a polarized human intestinal epithelial cell line: role of vesicular traffic. *J. Cell Biol.* **117**, 1197–1209 (1992).
51. McLaughlin-Drubin, M.E. & Munger, K. Biochemical and functional interactions of human papillomavirus proteins with polycomb group proteins. *Viruses* **5**, 1231–1249 (2013).
52. Warke, R.V. *et al.* Efficient dengue virus (DENV) infection of human muscle satellite cells upregulates type I interferon response genes and differentially modulates MHC I expression on bystander and DENV-infected cells. *J. Gen. Virol.* **89**, 1605–1615 (2008).
53. Furlong, D.B., Nibert, M.L. & Fields, B.N. Sigma 1 protein of mammalian reoviruses extends from the surfaces of viral particles. *J. Virol.* **62**, 246–256 (1988).

54. Sabin, A.B. Research on dengue during World War II. *Am. J. Trop. Med. Hyg.* **1**, 30–50 (1952).
55. Lambeth, C.R., White, L.J., Johnston, R.E. & de Silva, A.M. Flow cytometry-based assay for titrating dengue virus. *J. Clin. Microbiol.* **43**, 3267–3272 (2005).
56. Becavin, C. *et al.* Comparison of widely used *Listeria monocytogenes* strains EGD, 10403S, and EGD-e highlights genomic differences underlying variations in pathogenicity. *MBio* **5**, e00969–14 (2014).
57. Amit, I. *et al.* Unbiased reconstruction of a mammalian transcriptional network mediating pathogen responses. *Science* **326**, 257–263 (2009).

doi:10.1038/ni.2915